purified Tcp pilus and an antiserum raised against the denatured 20.5-kD pilin subunit of Tcp [See R. K. Taylor *et al.* in (*21*)].
25. Antisera to the two Tcp preparations (*23*) did not cross-react with BFP when tested by enzyme-linked immunosorbent assay (ELISA) and immunogold labeling microscopy.
26. The *tcpA* and *toxR* gene probes (1-kbp long) were prepared from *V. cholerae* strain 0395 as described by R. K. Taylor *et al.* (*21*). Hybridization of DNA prepared from each of the tested EPEC strains with the *tcpA* and *toxR* gene probes was performed under low- and high-stringency conditions.
27. A. S. Y. Ho, T. A. Mietzner, A. J. Smith, G. K. Schoolnik, *J. Exp. Med.* **172**, 795 (1990).
28. J. Swanson, S. Bergstrom, O. Barrera, K. Robbins, D. Corwin, *ibid.* **162**, 729 (1985).
29. After the adherence assay, 300 μl of a 1:1000 dilution in DMEM of the specific BFP antibody were added to the infected monolayers. After 30 min incubation at room temperature the cells were washed five times with DMEM, and 300 μl of a 1:1000 dilution of antirabbit IgG fluorescein conjugate were added for 30 min at room temperature. The cells were washed as before, fixed with a mixture of ethanol and acetic acid (95:5) for 20 min at −20°C, and the slides then examined by fluorescence microscopy.
30. For the purification of BFP, EPEC strain B171 was grown overnight at 37°C on TSA containing 5% defibrinated blood and harvested into 0.065 M monoethanolamine buffer (MEB), pH 10.0. The bundles were detached from the bacterial cells by shearing three times (4000 rpm for 10 min) in an Omnimixer (Dupont Sorvall, Newton, CT). The bacterial cells were removed by centrifugation (23500*g* for 30 min), and the supernatant containing the bundles was collected. The bacterial pellet was suspended again in the same volume of MEB, stirred, and recentrifuged. The supernatants were then pooled, and the bundles were precipitated from solution by addition of ammonium sulfate to a final concentration of 50%. After centrifugation (28400*g* for 15 min) the sedimented bundles were resuspended in MEB at 4°C. The insoluble pellet obtained by centrifugation (20800*g* for 30 min) was resuspended in 8 ml of MEB and left overnight at 4°C. After centrifugation (5000*g* for 5 min) the bundles were recovered in the pellet and resuspended in MEB, yielding the purified pilus preparation depicted in Fig. 3. Protein concentration was estimated by the method of M. Bradford [*Anal. Biochem.* **72**, 248 (1976)].
31. U. K. Laemmli, *Nature* **227**, 680 (1970).
32. NH_2-terminal amino acid sequencing was performed with purified pilus protein as described (*26*). Abbreviations for the amino acid residues are as follows: A, Ala; C, Cys; D, Asp; E, Glu; F, Phe; G, Gly; H, His; I, Ile; K, Lys; L, Leu; M, Met; N, Asn; P, Pro; Q, Gln; R, Arg; S, Ser; T, Thr; V, Val; W, Trp; and Y, Tyr.
33. M. A. Hermodson, C. S. Chen, T. M. Buchanan, *Biochemistry* **17**, 442 (1978).
34. We thank S. Falkow, J. V. Varkila, and N. Verma for helpful discussions; C. L. Francis for providing strains E2348/69 and JPN-15; N. A. Stockbine for providing EPEC strains 5368-64 (128ab:H1), 2517-80 (142:H6), 3448-87 (0114:NM), and 659-79 (0119:H6); S. Giono for providing EPEC strains 6 (0111:B4) and 51 (055:B5); R. K. Taylor for providing antisera to the Tcp of *V. cholerae* and to its denatured subunit; K. Reich for performing DNA hybridization of EPEC strains with the *tcpA* and *toxR* gene probes; A. Smith and J. Kenny for performing amino acid sequencing; D. Corwin for performing the scanning electron microscopy studies; and B. Efron for the statistical analysis shown in Table 1. This study was supported in part by NIH grant DK 38707 and by a grant from The Rockefeller Foundation.

18 March 1991; accepted 21 May 1991

Treatment of Established Renal Cancer by Tumor Cells Engineered to Secrete Interleukin-4

PAUL T. GOLUMBEK, AUDREY J. LAZENBY, HYAM I. LEVITSKY, LIZ M. JAFFEE, HAJIME KARASUYAMA, MITZI BAKER, DREW M. PARDOLL*

The generation of antigen-specific antitumor immunity is the ultimate goal in cancer immunotherapy. When cells from a spontaneously arising murine renal cell tumor were engineered to secrete large doses of interleukin-4 (IL-4) locally, they were rejected in a predominantly T cell–independent manner. However, animals that rejected the IL-4–transfected tumors developed T cell–dependent systemic immunity to the parental tumor. This systemic immunity was tumor-specific and primarily mediated by CD8$^+$ T cells. Established parental tumors could be cured by the systemic immune response generated by injection of the genetically engineered tumors. These results provide a rationale for the use of lymphokine gene–transfected tumor cells as a modality for cancer therapy.

TUMOR IMMUNITY (*1*) IS DEPENDENT on the existence of antigens within tumors that can be recognized as foreign by the host immune response. Spontaneously arising tumors, in contrast to chemically or virally induced tumors, were thought to not express tumor-specific antigens that can elicit an immune response (*2*). Thus, researchers questioned the usefulness of immunotherapy experiments performed with tumors induced by carcinogens or viruses. However, because cancers arise from the accumulation of multiple mutational events within the same cell (*3*), peptides from the mutated proteins may bind to major histocompatibility complex (MHC) class I molecules (*4*). These peptides, unique to the tumor cells, may serve as targets for a specific cytotoxic T cell (CTL) response. CTLs can recognize peptides derived from point-mutated intracellular proteins for tumors rendered immunogenic by mutagen treatment (*5*). Tumors that are less immunogenic can also be recognized by MHC class I–restricted, CD8$^+$ cytotoxic T cells if the tumor cells are engineered by gene transfection to secrete interleukin-2 (IL-2) (*6*). The local secretion by tumor cells of a helper lymphokine critical for CTL activation appears to bypass a deficient helper T cell arm of the immune system.

We examined the immunologic consequences of introducing tumor cells engineered to secrete the helper lymphokine IL-4, which participates in the regulation of growth and differentiation of B cells and T cells and in the generation of CTLs (*7*). IL-4 induces different genes, such as lipase, in activated CTLs than IL-2 induces, and the difference correlates with increased lytic function (*8*). Because of questions about the antigenic status of chemically or virally induced tumors (*2*), we studied a spontaneously arising renal cell carcinoma derived from a BALB/c mouse. When small numbers of Renca cells (1×10^3) are injected into BALB/c mice, they are not rejected. When injected under the renal capsule, Renca displays a metastatic pattern similar to human renal cell carcinomas (*9*).

Renca tumor cells were transfected with a murine IL-4 cDNA in a bovine papilloma virus expression vector containing the hygromycin-resistance gene (*10*). Transfectants were selected in hygromycin, and

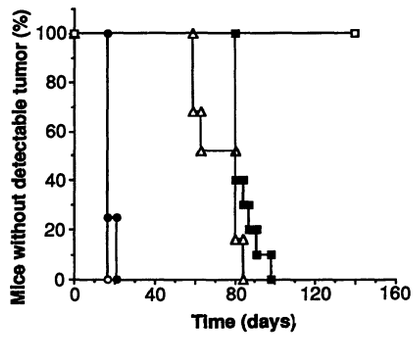

Fig. 1. Growth of Renca-TK and Renca–IL-4C in BALB/c wild-type, CB17 SCID and BALB/c nu/nu mice. BALB/c mice (10 per group) were injected subcutaneously with 1×10^6 cells on the left hind leg and tumor growth was observed. Tumor growth was assessed twice per week. As a control for potential effects of the vector sequences, the Renca-TK line was transfected with the identical PBCMG-neo vector as Renca–IL-4C, but with the HSV-TK gene instead of the IL-4 gene. ○, Renca-TK in SCID; ●, Renca-TK in BALB/c; □, Renca–IL-4C in BALB/c; △, Renca–IL-4C in SCID; and ■, Renca–IL-4C in nude.

P. T. Golumbek, H. I. Levitsky, L. M. Jaffee, M. Baker, D. M. Pardoll, Department of Medicine, Johns Hopkins University, Baltimore, MD 21205.
A. J. Lazenby, Department of Pathology, Johns Hopkins University, Baltimore, MD 21205.
H. Karasuyama, Department of Immunology, University of Tokyo, Tokyo, Japan.

*To whom correspondence should be addressed.

clones were assayed for their ability to secrete bioactive IL-4. The highest producing clone, Renca–IL-4C, secreted 1500 units/day per 10^5 cells as assayed on the IL-4–sensitive CT4S line (*11*) and was studied further. In vitro, Renca–IL-4C had identical morphology, growth kinetics, and MHC expression to parental Renca, indicating that IL-4 does not have any direct cytotoxic or cytostatic effects on the tumor. When Renca–IL-4C cells were injected subcutaneously into BALB/c mice, they were completely rejected even at large doses of cells (up to 2×10^7, Fig. 1). To determine whether lymphoid cells were involved in the local antitumor response, we injected Renca–IL-4C cells into BALB/c mice carrying either the nude (no T cells) or SCID (no T cells or B cells) mutation, no growth was seen for the first 2 months, but tumors eventually grew in all animals, indicating T cells were important for the ultimate elimination of the Renca–IL-4C tumor cells.

Histologic examination of the injection site of Renca–IL-4C in BALB/c mice demonstrated an influx of macrophages and some granulocytes (Fig. 2, A to C), with margination of granulocytes and macrophages on the endothelium of peri- and intratumor veins and venules (Fig. 2B). According to electron micrographic analysis, the macrophages had ruffled cell membranes and large amounts of endoplasmic reticulum and Golgi apparatus, characteristic of activation. The granulocytes contained major basic protein crystals, indicating that they were eosinophils. The predominant macrophage infiltrate in Renca–IL-4C contrasts with that of Renca–IL-2 transfectants, which are predominantly infiltrated with T lymphocytes. Renca tumor cells transfected with the same expression vector but carrying a control gene, herpes simplex virus-1 thymidine kinase (HSV-TK), grew identically to parental Renca in BALB/c mice and induced no local inflammatory response. Systemic administration of antibody to IL-4 resulted in growth of Renca–IL-4C tumors in BALB/c mice (*12*). Thus, IL-4 induced the inflammatory response and prompted the rejection of Renca–IL-4C cells. The response was similar to a report with plasmacytoma and breast carcinoma lines engineered to secrete IL-4, in which neither evidence for local infiltration of T cells at the tumor site nor a systemic immune response was detected (*13*). However, immunoperoxidase staining of our Renca–IL-4C tumors showed that, although few T cells enter the tumor site within the first 5 days after injection, they infiltrate by the second week (Fig. 2, D and E).

We next investigated whether the infiltrating T cells in the Renca–IL-4C tumor can recirculate and provide systemic immunity to parental, nontransfected Renca tumor cells (Fig. 3A). BALB/c mice immunized with Renca–IL-4C efficiently rejected parental Renca challenges (1×10^5 cells) at a distant site. When $CD8^+$ cells were eliminated before immunization, parental Renca challenges could not be rejected. Elimination of $CD4^+$ cells had a much lesser effect: some late recurrences in the CD4-depleted mice suggest the participation of $CD4^+$ cells in long-term "memory" responses. Thus, although the local rejection of Renca–IL-4C was predominantly mediated by non–T cells, systemic immunity against the wild-type challenge was dependent on $CD8^+$ T cells. Systemic immunity was not caused by circulating IL-4 or antibodies, because neither was detectable in the serum of these mice. Histologic analysis of the rejecting challenge tumors revealed that, in contrast to the immunization site, $CD3^+$ T cells were a major component of the infiltrating population during the early stages of rejection (Fig. 2, F to I). The tumor-reactive T cells induced by Renca–IL-4C circulated systemically and were present in the spleens of mice immunized with Renca–IL-4C. Splenocytes lysed ^{51}Cr-labeled Renca target cells (Fig. 3B). Most of the lysis was blocked by antibodies to CD8 but not to CD4, indicating most of the lysis was mediated by classical $CD8^+$ CTLs.

To determine whether the systemic CD8-dependent immune response was antigen-specific, we immunized mice with either Renca–IL-4C alone, Renca–IL-4C mixed at a 10:1 ratio with nontransfected cells of a second BALB/c–derived tumor (the colon tumor CT26), or CT26–IL-4B (CT26 line transfected with the same IL-4 expression vector and producing equal amounts of IL-4 as Renca–IL-4C). These mice were then challenged at a distant site with CT26 tumor cells (Fig. 4A). Almost all the BALB/c mice immunized with Renca–IL-4C alone did not reject the CT26 challenge. However, BALB/c mice immunized with CT26–IL-4B or with the CT26 cells mixed into the Renca–IL-4C inoculation were able to reject CT26 challenges. When mice were immunized with the same numbers of Renca–IL-4C and CT26 wild-type cells but at different sites rather than mixed in the same inocu-

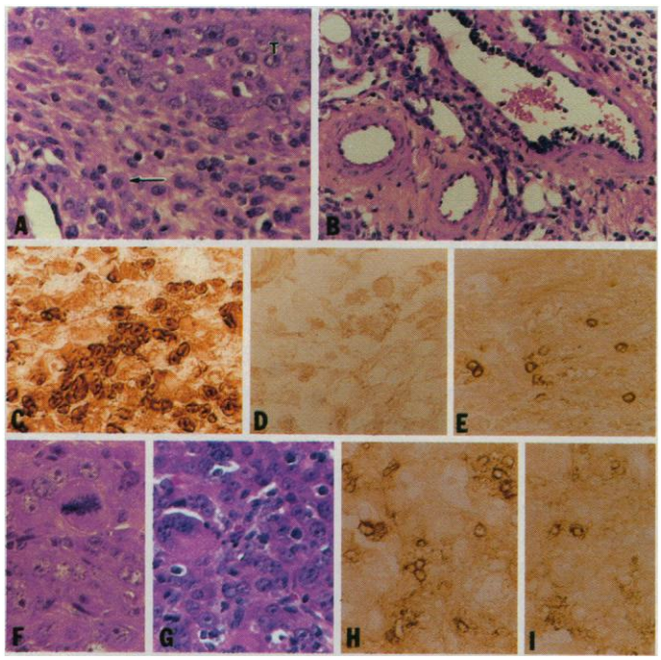

Fig. 2. Histologic analysis of injection sites of IL-4 transfected or parental Renca tumor. (**A**) Renca–IL-4C, hematoxylin and eosin, showing infiltrating macrophages (arrows) and eosinophils adjacent to the tumor mass (T). (**B**) Renca–IL-4C, hematoxylin and eosin, showing margination and transmigration of granulocytes through the endothelium of a small vein. (**C**) Renca–IL-4C, Mac-1 immunoperoxidase, confirming identity of infiltrating macrophages. (**D**) Renca–IL-4C, CD3 immunoperoxidase at 3 days after injection, showing absence of infiltrating T cells. (**E**) Renca–IL-4C, CD3 immunoperoxidase at 10 days after injection, showing increasing numbers of infiltrating T cells. (**F**) Parental Renca from a nonimmunized mouse, hematoxylin and eosin, demonstrating very rare infiltrating inflammatory cells. (**G**) Parental Renca from a mouse immunized 2 weeks earlier with Renca–IL-4C, hematoxylin and eosin, showing large numbers of infiltrating lymphocytes. (**H**) Parental Renca from a mouse immunized 2 weeks earlier with Renca–IL-4C, CD3 immunoperoxidase, confirming that the infiltrating lymphocytes are T cells. (**I**) Parental Renca from a mouse immunized 2 weeks earlier with Renca–IL-4C, CD8 immunoperoxidase, demonstrating that many of the T cells are $CD8^+$. Magnification on (A) and (C to I) ×400, on (B) ×160. Tumor cells were injected subcutaneously as in Fig. 1. Hematoxylin and eosin sections were fixed in 10% formalin and embedded in paraffin wax. For immunoperoxidase staining, tissue blocks were imbedded in OCT and snap frozen in liquid N_2. Frozen sections were fixed in acetone, blocked with goat or rat serum, incubated for 45 min with primary monoclonal antibody (MAb), washed in phosphate-buffered saline, and then stained with biotinylated secondary antibody (rabbit anti-rat for Mac-1 and CD8 stains, goat anti-hamster for CD3 stain). Localization of the antigen-antibody complexes was then done with Vectastain ABC (Vector labs) and diaminobenzidine developer. Primary MAbs were M1/70 [rat antibody to mouse CD3 (*16*)] 53-6.7 [rat antibody to CD8, (Becton Dickinson Immunocytometry Systems)], and 500A.2 [hamster antibody to mouse $CD3_\epsilon$ chain (*17*)].

lum, systemic immunity against CT26 did not develop. In the crisscross experiment (Fig. 4B), BALB/c mice rejected a parental Renca challenge after Renca–IL-4C immunization but not after CT26–IL-4B immunization. The CT26–IL-4A line, which produces 2% of the IL-4 CT26–IL-4B produces, was not completely rejected and did not induce systemic immunity to a parental CT26 challenge (*14*). These data show that the immune response generated by tumors producing IL-4 locally is tumor antigen-specific, critically dependent on the amount of local IL-4 production, and requires the antigen at the site of IL-4 production.

In animal models, although tumor vaccines can protect against challenges with limited numbers of tumor cells, the vaccines have not in general been able to cure animals of established tumors (*1*). We therefore determined whether Renca–IL-4C injections at a distant site could cure BALB/c mice that had established wild-type tumors (Fig. 5). Long-term cures (>160 days) could be obtained when mice were treated with Renca–IL-4C beginning 6 or 9 days after the introduction of wild-type Renca tumor cells. Histologic examination of Renca wild-type challenge sites confirmed that by 6 days after injection the tumor had invaded surrounding tissues, was vascularizing, and therefore met the standard pathologic criterion for an established tumor when Renca–IL-4C therapy was started. Also, when the cured mice were reinjected with parental Renca after 100 days, about 50% rejected the challenge (*14*), indicating some level of immune memory had been generated.

Our results demonstrate that poorly immunogenic, spontaneous tumors engineered to secrete IL-4 at high local concentrations can generate tumor-specific $CD8^+$ cytotoxic T cells in vivo capable of producing systemic immunity against the nontransfected tumor present at distant sites. The inflammatory infiltrate in the IL-4–transfected tumors is different from that of IL-2–transfected tumors. Although IL-2 transfectants result in a massive lymphocytic infiltrate, the predominant infiltrate in the IL-4 transfectants consists of activated macrophages. This finding and the partial dependence of the systemic immune response on $CD4^+$ cells suggest that an important role for IL-4 is the recruitment of antigen-presenting cells and consequent enhancement of tumor antigen presentation.

The ability of the systemic immune response generated by the IL-4 transfectants to cure animals of established tumors provides a basis for the application of lymphokine gene–transduced tumor cells as a therapeutic approach for human cancer. One of the critical features of this approach is that the lymphokine is produced only at the tumor site, thereby producing a strong immune response with no systemic toxicity. The extension of this strategy to human cancer therapy will require gene transfer

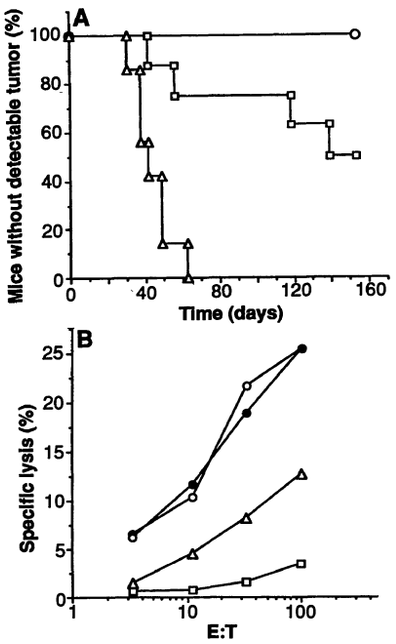

Fig. 3. Immunity against Renca cells induced by immunization with Renca–IL-4C is dependent on $CD8^+$ T cells. (**A**) BALB/c mice (10 to 15 per group) that were either not depleted, depleted of $CD4^+$ cells, or depleted of $CD8^+$ cells were immunized with 1×10^6 Renca–IL-4C cells in the left hind leg and then challenged 2 weeks later with 1×10^5 parental Renca cells in the right hind leg. Tumor growth on the challenge side was assessed twice per week. ○, no depletion; □, CD4 depletion; and △, CD8 depletion. (**B**) 1×10^6 Renca–IL-4C cells were injected subcutaneously into the left flank of BALB/c mice (three per group). After 2 weeks, pooled splenocytes from Renca–IL-4C–immunized or from unimmunized animals were removed and cultured for 5 days with mitomycin C–treated Renca cells in the presence of IL-2. At the end of culture, live cells were mixed with ^{51}Cr-labeled Renca targets at different effector-to-target ratios in an 8-hour ^{51}Cr release assay. Also shown are anti-CD4 and anti-CD8 blocking of Renca lysis by splenocytes from mice immunized with Renca–IL-4C. In vivo antibody depletions were started 4 weeks before injection of the Renca–IL-4C tumor. MAb GK1.5 (*18*) was used for CD4 depletions and MAb 2.43 (*19*) was used for CD8 depletions. Ammonium sulfate–purified ascites (0.1 ml per mouse; titered at >1:2000 by flow cytofluorometry of thymocytes) was injected intraperitoneally every other day for the first 3 weeks and then twice per week afterward. Depletion of T cell subsets was assessed on the day of tumor injections, 3 and 5 weeks after tumor injection by flow cytometric analysis. The CTL experiment is representative of three independent studies. Assays were performed as described (*4*). Percent specific lysis ($cpm_{exp} - cpm_{min}/cpm_{max} - cpm_{min} \times 100$) is plotted on the y-axis for various effector-to-target ratios (E:T). For antibody blocking, a 1:200 dilution of ammonium sulfate cut preparations of GK1.5 and 2.43 were added to microwells at the start of ^{51}Cr release assays. ●, Renca–IL-4C, no block; ○, Renca–IL-4C, CD4 block; △, Renca–IL-4C, CD8 block; □, unimmunized, no block.

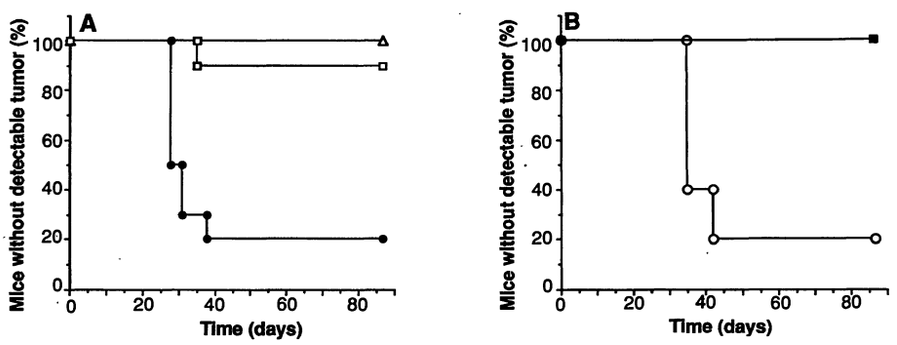

Fig. 4. Systemic protection induced by local IL-4 production is tumor-specific. (**A**) BALB/c mice (10 per group) were immunized subcutaneously in the left hind leg with either 1×10^6 Renca–IL-4C cells, 1×10^6 Renca–IL-4C cells mixed with 1×10^5 wild-type CT26 cells, or 1×10^6 CT26–IL-4B cells. Two weeks later they were challenged with 1×10^5 wild-type CT26 cells. Groups were immunized as follows: △, Renca–IL-4C + CT26 10:1; □, CT26–IL-4B; ●, Renca–IL-4C. (**B**) BALB/c mice were immunized subcutaneously in the left hind leg with either 1×10^6 CT26–IL-4B cells or Renca–IL-4C cells. Two weeks later, they were challenged with 1×10^5 parental Renca cells. Growth at the challenge site was assessed twice a week. Groups were immunized as follows: ■, Renca–IL-4C; ○, CT26–IL-4B.

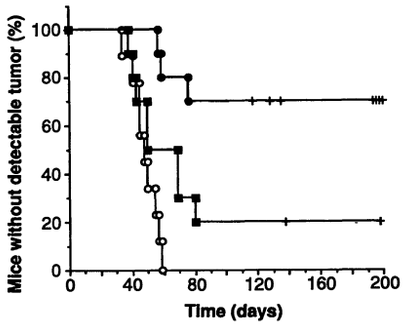

Fig. 5. Injection of Renca–IL-4C cells can cure animals with small amounts of established parental tumor at a distant site. BALB/c mice (10 per group) were injected subcutaneously in the right hind leg with 1×10^4 Renca wild-type cells. After 6 or 9 days, they were given three weekly injections of 1×10^6 Renca–IL-4C cells subcutaneously in the left hind leg. Growth at the challenge site was assessed twice per week. ●, day 6; ■, day 9; ○, control.

systems capable of introducing lymphokine genes into primary human tumor explant cultures established at the time of surgery. The development of high-efficiency retroviral vectors (*15*) makes this feasible.

REFERENCES AND NOTES

1. J. Marx, *Science* **244**, 813 (1989); G. Mathe, *Adv. Cancer Res.* **14**, 1 (1971).
2. H. B. Hewitt, E. R. Blake, E. S. Walder, *Br. J. Cancer* **33**, 241 (1976).
3. A. M. Townsend *et al.*, *Cell* **44**, 959 (1986); J. L. Maryanski, P. Pala, J. Corradin, B. B. Jordan, J. C. Cerrotini, *Nature* **324**, 578 (1986); M. M. Moore, F. R. Carbone, M. J. Bevan, *Cell* **54**, 777 (1988).
4. E. R. Fearon and B. V. Vogelstein, *Cell* **61**, 759 (1990).
5. C. Lurquin *et al.*, *ibid.* **58**, 293 (1989).
6. E. R. Fearon *et al.*, *ibid.* **60**, 397 (1990).
7. W. E. Paul and J. Ohara, *Annu. Rev. Immunol.* **5**, 429 (1987); R. Fernandez-Botran *et al.*, *Proc. Natl. Acad. Sci. U.S.A.* **83**, 9689 (1986); J. Hu-Li *et al.*, *J. Exp. Med.* **165**, 157 (1987); M. Widmer and K. Grabstein, *Nature* **326**, 795 (1987); G. Trenn, H. Takayama, J. Hu-Li, W. E. Paul, M. V. Sitkovsky, *J. Immunol.* **140**, 1101 (1988).
8. M. J. Grusby *et al.*, *Cell* **60**, 451 (1990).
9. G. P. Murphy and W. J. Hrushesky, *J. Natl. Cancer Inst.* **50**, 1013 (1973); R. R. Salup, R. B. Herberman, R. H. Wiltrout, *J. Urol.* **134**, 1236 (1985).
10. DNA was introduced into cells as a coprecipitate with calcium phosphate [F. L. Graham and A. J. van der Eb, *Virology* **52**, 456 (1973); M. Wigler *et al.*, *Proc. Natl. Acad. Sci. U.S.A.* **76**, 1373 (1979)]. The Renca–IL-4C cell line was obtained by transfection with 5 μg of the plasmid vector pBCMG-hygro–IL-4, a bovine papilloma virus expression vector containing a murine IL-4 cDNA clone under the transcriptional control of a cytomegalovirus promoter with a rabbit beta-globin intron, splice, and poly(A) addition signals; it also contains the hygromycin-resistance gene [H. Karasuyama and F. Melchers, *Eur. J. Immunol.* **18**, 97 (1988)]. The CT26–IL-4A line was derived in the same way. CT26–IL-4B was derived from CT26–IL-4A by an additional selection step in hygromycin (4 mg/ml) to generate a line that secreted similar amounts of IL-4 as Renca–IL-4C.
11. Supernatants of transfected cells (5×10^5 cells per well plated in a 24-well plate with 1.5 ml of media for 24 hours) were assayed for IL-4 by transferring dilutions of tumor cell–conditioned media to 96-well microtiter plates containing 3000 CT4S cells per well. After 48 hours, ^{3}H-thymidine was added for 12 hours after which incorporation was assessed with a PHD cell harvester. Units per milliliter of IL-4 were calculated as the reciprocal of the supernatant dilution giving half-maximal proliferation of CT4S.
12. Anti–IL-4 treatments were done with 1 mg of 11B11 MAb [J. Ohara and W. E. Paul, *Nature* **315**, 333 (1985)] injected intraperitoneally three times per week.
13. R. I. Tepper, P. K. Pattengale, P. Leder, *Cell* **57**, 503 (1989).
14. P. Golumbek and D. Pardoll, unpublished data.
15. R. Mann, R. C. Mulligan, D. Baltimore, *Cell* **33**, 153 (1983); R. C. Mulligan, in *Etiology of Human Disease at the DNA Level*, J. Lindsten and U. Petterson, Eds. (Raven, New York, 1991), p. 143.
16. T. M. Springer, G. Galfre, D. S. Secher, C. Milstein, *Eur. J. Immunol.* **9**, 301 (1979).
17. W. L. Havran *et al.*, *Nature* **330**, 170 (1987).
18. D. M. Dialynas *et al.*, *J. Immunol.* **131**, 2445 (1983).
19. M. Sarmiento, A. Glasebrook, F. Fitch, *J. Immunol.* **125**, 2665 (1980).

20. We thank G. Dranoff, R. Mulligan, W. Paul, B. Vogelstein, E. Fearon, J. Simons, and M. Howard for advice. Supported in part by the M. L. Smith Charitable Trust. D.M.P. is a recipient of the Cancer Research Institute–Benjamin Jacobson Family Investigator Award and the RJR Nabisco Research Scholars Award.

17 June 1991; accepted 9 September 1991

Functional Mapping of the Human Visual Cortex by Magnetic Resonance Imaging

J. W. BELLIVEAU,* D. N. KENNEDY, R. C. MCKINSTRY, B. R. BUCHBINDER, R. M. WEISSKOFF, M. S. COHEN, J. M. VEVEA, T. J. BRADY, B. R. ROSEN

Knowledge of regional cerebral hemodynamics has widespread application for both physiological research and clinical assessment because of the well-established interrelation between physiological function, energy metabolism, and localized blood supply. A magnetic resonance technique was developed for quantitative imaging of cerebral hemodynamics, allowing for measurement of regional cerebral blood volume during resting and activated cognitive states. This technique was used to generate the first functional magnetic resonance maps of human task activation, by using a visual stimulus paradigm. During photic stimulation, localized increases in blood volume (32 ± 10 percent, $n = 7$ subjects) were detected in the primary visual cortex. Center-of-mass coordinates and linear extents of brain activation within the plane of the calcarine fissure are reported.

PHYSIOLOGICAL, ANATOMICAL, AND cognitive psychophysical studies indicate that the brain possesses anatomically distinct processing regions (*1, 2*). During cognitive task performance, local alterations in neuronal activity induce local changes in metabolism and cerebral perfusion [blood flow and, as shown here, blood volume (*3*)]. These changes can be used to map the functional loci of component mental operations (*4*). Because the cerebral hemodynamic state in nonactivated brain areas is quite stable over time, a resting-state perfusion image can be subtracted from a stimulated-state image to create a new functional map depicting local changes caused by the activation task (*5*). To date, these functional maps have relied on radionuclide techniques [primarily positron emission tomography (PET)] that suffer from limited spatial and temporal resolution. Although accurate center-of-mass coordinates of activated regions have been obtained, the extent of cortex involved in a given task cannot be determined precisely, and distributed regions separated by less than the full width at half maximum (FWHM) resolution of the instrument cannot be resolved individually (*6*). In comparison, nuclear magnetic resonance (NMR) imaging (or MRI) is a high-resolution in vivo method for studying human cerebral anatomy (7). Recent advances in scanning speed, coupled with approval of contrast agents for human use, have yielded NMR techniques for quantitative imaging of cerebral blood volume (CBV) (*8*).

We investigated the human visual cortex using photic stimulation, a robust stimulus that produces regional changes in cerebral blood flow (CBF) of at least 30 to 50% (*5, 9*). Dynamic susceptibility–contrast NMR imaging of an intravenously administered paramagnetic contrast agent [0.5 M, gadolinium diethylenetriaminepentaacetic acid, Gd(DTPA)$^{2-}$] was used to produce regional CBV maps of the human brain during resting and activated states (*8, 10*). CBV maps were correlated directly to high-resolution (T1-weighted) three-dimensional (3-D) images of the underlying anatomy, allowing for precise determination of gray-white matter boundaries and activated-nonactivated borders. Functional CBV and anatomic data sets were translated into proportionately measured stereotactic coordinates relating to the line between the anterior and posterior commissures (AC-PC line) (*11*). This translation allows direct correlation to reported standardized PET maps of the visual cortex (*5, 9*).

Seven normal subjects underwent dynamic NMR imaging with a prototype high-speed imaging device (1.5-T GE Signa, modified by Advanced NMR Systems, Inc., Wilmington, MA) based on a variation of the echo planar imaging (EPI) technique first described by Mansfield [in (*12*)]. Light-proof, patterned-flash stimulating goggles (Model S10VS, Grass Instruments, Quincy, MA) were placed over the subject's eyes. The stimulus rate was fixed for predicted maximum CBF response (*5*) at 7.8 Hz. A snugly fitting head holder was used to minimize subject movement between scans. A surface radio frequency (r.f.) coil over the occipital pole was used to improve signal-to-noise over the posterior half of the brain.

J. W. Belliveau, R. C. McKinstry, B. R. Buchbinder, R. M. Weisskoff, M. S. Cohen, J. M. Vevea, T. J. Brady, B. R. Rosen, Massachusetts General Hospital–NMR Center, Department of Radiology, Massachusetts General Hospital and Harvard Medical School, Boston, MA 02114.

D. N. Kennedy, Massachusetts General Hospital–NMR Center, Departments of Radiology and Neurology, Massachusetts General Hospital and Harvard Medical School, Boston, MA 02114.

*To whom correspondence should be addressed, at Massachusetts General Hospital–NMR Center, 13th Street, Charlestown, MA 02129.